Received: 25 June 2020 | Revised: 15 September 2020 | Accepted: 16 September 2020

DOI: 10.1002/qua.26523

FULL PAPER

International Journal of QUANTUM CHEMISTRY WILEY

Bypassing the multireference character of singlet molecular oxygen, part 1:1,4-cyclo-addition

Malte F. Jespersen | Solvejg Jørgensen | Matthew S. Johnson | Kurt V. Mikkelsen

Department of Chemistry, University of Copenhagen, Copenhagen, Denmark

Correspondence
Kurt V. Mikkelsen, Department of Chemistry, University of Copenhagen, Universitetsparken 5, DK-2100 Copenhagen, Denmark.
Email: kmi@chem.ku.dk

Abstract

Modeling reactions involving singlet molecular oxygen (O_2 [$^1\Delta_g$]) is challenging because the degeneracy of the highest occupied molecular orbital and lowest unoccupied molecular orbital (HOMO and LUMO) orbitals of oxygen causes a significant multireference character. Within the limit that singlet-singlet near-degeneracy disappears in the transition state, it would be possible to bypass singlet oxygen's multireference character by simply adding the experimentally determined singlet/triplet splitting (22.5 kcal/mol) to the energy of the triplet ground state of molecular oxygen. This method is tested by calculating rate constants for the reactions of singlet molecular oxygen with furan, 2-methylfuran, 2,5-dimethylfuran, pyrrole, 2-methylpyrrole, 2,5-dimethylpyrrole, and cyclopentadiene using transition state theory. We find that the reaction rate coefficients are within a factor of 15 of experimentally determined rate constants, indicating an error in the barrier energy of roughly 3 kcal/mol. Furthermore, we find that energy refinement at the CCSD(T)-F12 level of theory is crucial to achieving accurate results. We conclude that, based on a comparison with an experiment, this approximation is valid to some degree and can be used for other systems involving the 1,4-cyclo-addition of singlet oxygen.

KEYWORDS

CCSD(T)-F12, reaction rate, singlet molecular oxygen, Singlet/Triplet splitting

1 | INTRODUCTION

Molecular oxygen plays an extremely important role in all aspects of aerobic life on earth, and its chemistry is closely related to the electronic structure of molecular oxygen.[1,2] Molecular oxygen has three electronic states that, in terms of energy, are located very close to one another. In vacuum, the transitions between the electronic states of molecular oxygen in vacuum are forbidden by selection rules related to symmetry, spin, orbital angular momentum, and parity.[3] The lowest-lying singlet state of molecular oxygen ($^1\Delta_g$) has a lifetime that is long enough to undergo chemical reactions. The reactivity of singlet oxygen is used in many applications, such as removing pollutants from waste water,[4,5] in photodynamic therapy for treating cancer,[6,7] and as a valuable selective oxidant in organic chemistry.[7,8] Furthermore, a reaction with singlet oxygen could be an important oxidation path for certain species in the atmosphere and hydrosphere.[9]

Ab initio calculations with systems involving singlet oxygen are challenging due to their inherent multireference character, caused by the degeneracy of the HOMO and LUMO orbitals in singlet oxygen. These systems have been the subject of many theoretical studies.[10–14] CASSCF provides a direct way of including the static correlation of the system.[15] CASSCF calculations require the selection of an active space that includes the orbitals involved in the reaction. The CASSCF method primarily describes the static correlation of the system. Addition of a dynamic correlation to a CASSCF wavefunction is challenging because of its high computational cost and poor scaling with size. Another approach to describing the multireference character of singlet oxygen is the approximate spin projection method, where the HOMO and LUMO orbitals are

allowed to mix, and the electronic energy is corrected on the basis of the spin contamination and the energy of the first spin contaminant. The spin contamination error can be reduced by using approximate spin projection methods[16]; however, with density functional theory (DFT), the results are sensitive to the choice of functional.[17–19]

An alternative approach would be to bypass the multireference character of singlet oxygen by performing the electronic structure calculation using ground-state triplet molecular oxygen and then adding the experimentally determined energy splitting between the triplet and singlet states of molecular oxygen, as illustrated in Figure 1. For the reaction of singlet oxygen with cyclohexadiene,[20] this approach has been shown to yield the same qualitative results for B3LYP/6-31G(d) as those of refining the electronic energy with CASPT2(12e,10o)/6-31G(d). The accuracy of this approach depends on whether the multireference character persists in the transition state (TS). While the degeneracy of the HOMO and LUMO orbitals in the singlet oxygen moiety is most likely lost in the TS, the TS might still possess a multireference character due to close lying molecular orbitals. While bypassing the multireference character is by far the most simple and straightforward approach for treating systems containing singlet oxygen, the approach relies on the TS being well behaved, without a significant multireference character.

1.1 | Discussion of the mechanism

Singlet oxygen is reactive toward many compounds, including alkenes and sulfides. For an alkene that is a conjugated diene in the *cis* conformation, singlet oxygen may undergo a 1,4-cyclo-addition to the alkene via the Diels Alder mechanism to form an endoperoxide, as illustrated in Figure 2. Whether the 1,4-cyclo-addition mechanism of singlet oxygen occurs in a single concerted reaction or as a stepwise addition with a stable intermediate has been debated.[21] Bobrowski et al. examined the 1,4-cyclo-addition of singlet oxygen to benzene and *cis*-butadiene and found that the benzene reaction progresses through a concerted mechanism, while the *cis*-butadiene reaction proceeds via a stepwise addition, in agreement with earlier MINDO/3 studies.[14] The stepwise mechanism proceeded via a biradical intermediate calculated at the MCQDPT2/6-31G*//

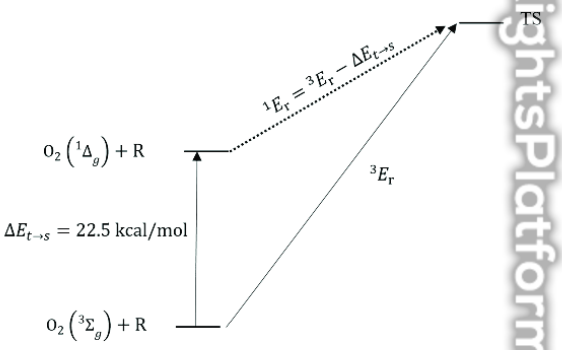

FIGURE 1 Illustration of the calculations needed to bypass the multireference character of singlet oxygen

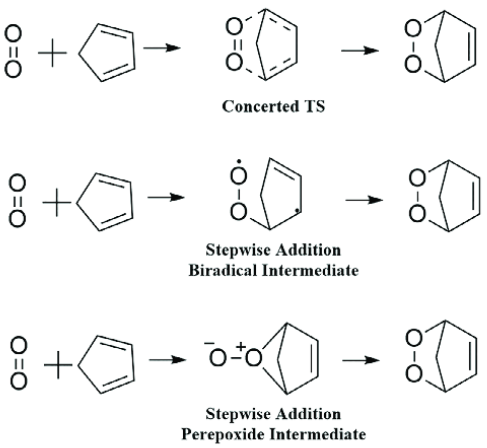

FIGURE 2 The 1,4-cyclo-addition mechanism for the reaction between singlet oxygen and cyclopentadiene

MCSCF/6-31G* level. The concerted mechanism was found to have a second-order saddle point 1 kcal/mol above the stepwise TS.[22] However, earlier studies at the MP2/6-31G*//HF/3-21G level of theory found a first-order saddle point along the concerted path to be the lowest for the cyclo-addition of *cis*-butadiene and singlet oxygen.[23] Sevin et al. studied the cyclo-addition of singlet oxygen to 1,3-cyclohexadiene at the CASPT2(12e,10o)/6-31G(d)//B3LYP/6-31G(d) level of theory.[20] In this study, the initial energy barrier was found to be 6.5 kcal/mol. They found that, while the reaction takes place via a two-step mechanism at the DFT level, the energy barrier of the second TS becomes negative at the CASPT2 level, transforming the mechanism into a concerted but nonsynchronous process. Fudickar and Linker found that the reactions of singlet oxygen with anthracenes shift from a stepwise mechanism to a concerted one on going from the gas phase to acetonitrile solution,[24] reflecting the close competition between the two reaction channels. An experimental investigation by Gorman et al. found a concerted mechanism for the reaction between singlet oxygen and a range of cyclodienes in toluene.[25] There is experimental evidence that the cyclo-addition reaction in a solvent involves a reversibly formed exiplex that might become rate-determining at low temperatures.[26]

The goal of this paper is to evaluate different strategies for calculating accurate energy barriers for reactions involving singlet oxygen. Two strategies have been tested. In the first, we bypass the multireference character of singlet oxygen by performing the energy calculation on the triplet state and then adding the experimentally determined energy difference of 22.5 kcal/mol. The second uses the broken symmetry solution of an unrestricted DFT calculation (UDFT), where the spin contamination is removed using the approximated spin-projected method (AP-UDFT) proposed by Yamaguchi and coworkers.[16]

The resulting energy barriers are used to calculate the rate constants with TS theory (TST). The calculated rate constants are compared with experimentally obtained rate constants to evaluate the energy barriers. We emphasize that, while TST is a simple approach, it provides valuable insight regarding the reaction kinetics, and it yields results that can be compared with the experiment. We note that, while the Arrhenius parameters for the reactions of furan, 2-methylfuran, and cyclopentadiene obtained by Ashford and Ogryzlo have similar pre-exponential factors but different activation energies, the different reactivities of these systems are only controlled by their activation energies. Based on this result, we argue that TST is a useful approach for testing the performance of different electronic structure theories. The simplicity of the TST model makes the calculation transparent. The calculated rate constants have an exponential dependency on the energy barrier, which makes the calculation very sensitive to this parameter. A change of 1 kcal/mol on the energy barrier leads to an approximately 5-fold change in the rate constant, which makes the calculated TST rate constants a useful tool in validating the quality of the energy barriers. A set of model systems consisting of furan, 2-methylfuran, 2,5-dimethylfuran, pyrrole, 2-methylpyrrole, 2,5-dimethylpyrrole, and cyclopentadiene is used to test the method. The test molecules have conjugated five-membered rings that are able to undergo 1,4-cyclo-addition with singlet oxygen. The gas-phase rate constants for furan, 2-methylfuran, 2,5-dimethylfuran, 2,5-dimethylpyrrole, and cyclopentadiene have all been determined experimentally[27–29] and serve as validations of the suggested computational strategy.

2 | COMPUTATIONAL METHOD

Gaussian 16[30] is used for all geometry optimizations, employing the aug-cc-pVTZ[31] (AVTZ) basis set and the ωB97XD,[32] B3LYP[33] and M06-2X[34] functionals. The strategy relying on the addition of the experimentally determined singlet/triplet splitting is based on geometry optimizations performed with UDFT and restricted density functional theory (RDFT) (restricted open density functional theory [RODFT] in the case of triplet oxygen), whereas the strategy based on spin projection is based on geometries optimized with UDFT. Intrinsic reaction coordinate calculations are performed to confirm that the TS connects the reactants to the products. Molpro 2012[35] is used to perform single-point RCCSD(T)-F12a/VDZ-F12[36] energy calculations for the obtained geometries. The basis set convergence of the RCCSD(T)-F12a method is tested by comparing the RCCSD(T)-F12a/VDZ-F12 and RCCSD(T)-F12a/VTZ-F12 single-point energies performed for the RωB97XD/AVTZ geometries of the furans. If a system possesses a significant multireference character, RCCSD(T)-F12a calculations might yield unreliable results because of the poor quality of the Hartree Fock (HF) reference wavefunction. For example, RCCSD(T)-F12a/VDZ-F12 predicts a singlet/triplet splitting for molecular oxygen of 28.51 kcal/mol, which is around 6 kcal/mol too high. Two markers are used to judge whether the multireference character is still pronounced in the TS, namely, the T_1 diagnostic obtained in the RCCSD(T)-F12a calculations and the spin contamination obtained either from UDFT optimization or from single-point UDFT calculations performed at the RDFT-optimized geometries. (10e,8o)CASPT2/AVTZ calculations are performed along the reaction coordinate of the furan and singlet molecular oxygen to obtain the energy of the two lowest singlet states and the triplet state. The (10e,8o)CASPT2/AVTZ calculations are performed in Molpro 2012.

The rate constants are calculated using TST:[37]

$$k = L\kappa\frac{k_B T}{h}\frac{Q_{TS}}{Q_R Q_{1O_2}} e^{-\frac{E_0}{k_B T}}$$

where k_B, T, and h are Boltzmann's constant, the temperature (298 K), and Planck's constant respectively; $\frac{Q_{TS}}{Q_R Q_{1O_2}}$ is the ratio of the partition functions for the TS and the two reactants; and E_0 is the electronic energy barrier, including the zero-point vibrational energy (ZPVE). κ is the tunneling

correction and is based on the one-dimensional Eckart tunneling correction, which is calculated from the imaginary frequency of the TS and the forward and reverse energy barriers.[38] L is the symmetry factor for the reaction and is described in greater detail in the Supporting Information.

3 | RESULT AND DISCUSSION

3.1 | Singlet/triplet splitting in singlet oxygen

It is well known that the singlet/triplet splitting of singlet oxygen is poorly described by a single reference method.[20] This fact is illustrated in Table 1, where RDFT is observed to overestimate the energy splitting by 12.7 kcal/mol, whereas UDFT underestimates the energy splitting by 10.92 kcal/mol. Even the CCSD(T)-F12a/VDZ-F12 method overestimates the energy barrier by around 6 kcal/mol. The UDFT wavefunction can be spin-contaminated, where higher spin states are mixed in the wavefunction. This is evident from the $\langle S^2 \rangle$ value, which is calculated to be around 1 for singlet oxygen, significantly deviating from the expected value of 0 for a pure singlet. Furthermore, the lowering of the singlet-triplet splitting from RDFT to UDFT can be attributed to spin contamination of the wavefunction, where the lower-lying triplet state is mixed into the UDFT wavefunction. The approximated spin-projection scheme provides a method for removing the contamination coming from the first spin contaminant.[16,17] As seen in Table 1, the approximated spin-projected value (AP-UωB97XD/AVTZ) agrees well with the experimentally determined value. The singlet/triplet splittings determined using AP-UDFT and calculated with the functionals B3LYP and M06-2X are shown in Table 1. The energy difference across all methods is 8.63 kcal/mol; in particular, M06-2X seems to perform poorly. The fact that M06-2X shows the worst performance is interesting as this functional has often been chosen for systems involving singlet oxygen using the approximated spin projection method.[18,39]

The large variation among the different DFT functionals indicates that care should be taken when selecting the DFT functional to be used with approximate spin projection methods.

3.2 | Furan, 2-methylfuran and 2,5-dimethylfuran

TS structures for the 1,4-cyclo-addition of singlet oxygen to furan, 2-methylfuran, and 2,5-dimethylfuran calculated at the ωB97XD/AVTZ level of theory are shown Figure 3. The TS structures are similar across the different DFT methods: The TS connects the reactants with the endoperoxide products in a concerted reaction, where both C-O bonds are formed simultaneously without a stable intermediate between reactants and products. Table 2 shows the energy barriers obtained by performing CCSD(T)-F12a/VDZ-F12 calculations using the optimized DFT geometries for the reactions of furan, 2-methylfuran, and 2,5-dimethylfuran with singlet oxygen. The calculated energy barriers vary within 1.59 kcal/mol across the different DFT methods, showing that similar structures are obtained for the different DFT methods.

Single-point CCSD(T)-F12a/VTZ-F12 calculations performed using the ωB97XD/AVTZ geometries are shown in Table 2: These calculations were used to test the effect of expanding the basis set. The energy barriers were seen to decrease by 0.31 kcal/mol or less as the size of the basis

	$\Delta E_{t \rightarrow s}$ $\left(\frac{\text{kcal}}{\text{mol}}\right)$
ROωB97XD/AVTZ	35.20
UωB97XD/AVTZ	11.58
AP-UωB97XD/AVTZ	23.16
AP-UB3LYP/AVTZ	20.12
AP-UM06-2X/AVTZ	28.75
UCCSD(T)-F12a/VDZ-F12	28.85
RCCSD(T)-F12a/VDZ-F12	28.51
Exp.	22.5

TABLE 1 Singlet/triplet splitting calculated using some single-reference methods

FIGURE 3 Transition state (TS) structures for the 1,4-cyclo-addition of singlet oxygen on furan (left), 2-methylfuran (middle), and 2,5-dimethylfuran (right), calculated at the RωB97XD/AVTZ level of theory

TABLE 2 Spin contaminations, T_1 diagnostic, and energy barriers including zero-point vibrational energy (ZPVE) in kcal/mol and rate constants in $\frac{cm^3}{s}$ calculated at CCSD(T)-F12a/VDZ-F12//DFT/AVTZ level of theory using the known singlet/triplet splitting in molecular oxygen

Furan + $^1O_2$	$\langle S^2 \rangle$	T_1	E_0 $(\frac{kcal}{mol})$	k $(\frac{cm^3}{s})$
RM06-2X	0.35	0.016	4.93	3.01×10^{-18}
UM06-2X	0.11	0.017	4.64	6.18×10^{-18}
RB3LYP	0.34	0.017	4.44	8.76×10^{-18}
UB3LYP	0.10	0.018	3.76	3.39×10^{-17}
RωB97XD	0	0.017	4.66	5.49×10^{-18}
RωB97XD[a]	0	0.017	4.35	9.29×10^{-18}
Exp.[27]				3.49×10^{-17}
2-Methylfuran +$^1O_2$	$\langle S^2 \rangle$	T_1	E_0 $(\frac{kcal}{mol})$	k $(\frac{cm^3}{s})$
RM06-2X	0.48	0.016	2.41	2.15×10^{-16}
UM06-2X	0.13	0.016	1.79	7.51×10^{-16}
RB3LYP	0.45	0.016	1.92	5.93×10^{-16}
UB3LYP	0.11	0.017	0.82	4.09×10^{-15}
RωB97XD	0	0.016	1.99	4.69×10^{-16}
RωB97XD[a]	0	0.016	1.71	7.58×10^{-16}
Exp.[27,28]				$(1.66\text{-}5.81)\times 10^{-16}$
2,5-Dimethylfuran +$^3O_2$	$\langle S^2 \rangle$	T_1	E_0 $(\frac{kcal}{mol})$	k $(\frac{cm^3}{s})$
RM06-2X	0.62	0.015	0.21	9.16×10^{-15}
UM06-2X	0.15	0.016	–0.98	6.22×10^{-14}
B3LYP	-	-	-	
RωB97XD	0	0.015	0.05	1.03×10^{-14}
RωB97XD[a]	0	0.015	–0.12	1.42×10^{-14}
Exp.[28]				2.49×10^{-14}

[a]Energies obtained from single-point CCSD(T)-F12a/VTZ-F12 calculations.

set increases. While some spin contamination was observed for the (U/R)B3LYP/AVTZ- and (U/R)M06-2X/AVTZ-optimized geometries, interestingly, no spin contamination was observed in the UωB97XD/AVTZ calculation using the RωB97XD/AVTZ-optimized geometry. This might indicate that ωB97XD is more robust in treating 1,4-cyclo-addition reactions. The T_1 diagnostics for the TSs shown in Table 2 are all lower than 0.02, which is a commonly accepted upper limit indicating the reliability of a single reference method.[40,41] As both the spin contamination and the T_1 diagnostics were sufficiently low, the CCSD(T)-F12a method was deemed to be satisfactory for improving the accuracy of the electronic energies of the DFT-optimized TS structures.

The calculated rate constants shown in Table 2 are about the same order of magnitude of the experimentally determined rate constants. Furthermore, rate constants calculated using the CCSD(T)/VTZ-F12 single-point energies perform slightly better than the ones calculated using the CCSD(T)/VDZ-F12 energies. The calculated rates are generally lower than the experimentally determined rates, which may be surprising as TST is normally expected to overestimate rate constants where tunneling is not important.[42] This observation might stem from use of the CCSD(T)-F12a/VDZ-F12 method, which consistently overestimates the energy in the TS region, which may indicate that some multireference character is still persistent in the TS region. Alternatively, the optimized DFT geometries may not accurately describe the true reaction coordinate, a possibility that is discussed later in this paper.

The experimentally determined rate constants are observed to increase in the order $k_{\text{furan}} < k_{\text{2-methylfuran}} < k_{\text{2,5-dimethylfuran}}$, a trend that is clearly captured in the theoretically determined rate constants. Two experimentally determined rate constants were found for 2-methylfuran; they differ by a factor of 4. If the factor of 4 is taken as a representative experimental uncertainty for these kinds of systems, the theoretically calculated rates are close to matching the experimental values. It should be mentioned that only standard TST calculations were performed on the chosen systems and that more advanced methods would be expected to improve the accuracy of the calculation.

Table S2 shows the energy barriers for the furans calculated using the approximate spin projection scheme and the bypassing method (without any CCSD(T)-F12a energy refinement). The energy barriers were compared to the CCSD(T)-F12a/VTZ-F12//RωB97XD/AVTZ results, which were seen to be in good agreement with the experiment, hence validating it as a benchmark value. The energy barriers are seen to vary within 8.35 and 3.02 kcal/mol across the different functionals using the approximate spin-projected and bypassing methods, respectively. A variation of 8.35 kcal/mol in the energy would lead to a change of the TST rate constant by a factor of 10^6, which is not acceptable. The lower fluctuation observed for the bypassing method indicates that this method is less sensitive to the selection of the DFT functional; however, the energy barriers are still 2.07 to 5.56 kcal/mol higher than the CCSD(T)-F12a/VTZ-F12//RωB97XD/AVTZ values. Hence, while the absolute values of the rate

constants are expected to be inaccurate, the relative values might still be accurate as all the calculated energy barriers are in qualitative agreement with the expected tendency $E_{0,(\text{furan})} > E_{0,(\text{2-methylfuran})} > E_{0,(\text{2,5-dimethylfuran})}$. The energy barriers calculated using AP-UM06-2X are within 1 kcal/mol of the energy barriers obtained at the CCSD(T)-F12a/VTZ-F12//RωB97XD/AVTZ level of theory, and the method is observed to be the best-performing method for predicting energy barriers for the 1,4-cyclo-addition if energy refinement at the CCSD(T)-F12 level is excluded.

T. Karsili et al. recently studied the 1,4-cyclo-addition reaction of singlet molecular oxygen.[43,44] They performed CASPT2 calculations on approximate reaction surfaces obtained from the linear interpolation of internal coordinates. Their calculations suggest that the two degenerate singlet states of molecular oxygen move away from one another in energy as the reaction proceeds toward the TS, which supports the logic of the bypassing scheme investigated in this study. In their study, the triplet and singlet surfaces were found to cross in the region near the TS. As the triplet surface is fully repulsive, surface hopping will lead to a quenching of the reaction; the quenching efficiency will be dependent on the spin-orbit coupling. Recent work from the group of Ogilby investigated the quenching mechanism in a solvent where crossing of the singlet and triplet surfaces was a key factor.[45] There are mechanistic similarities between quenching and chemical reaction, and the two processes are in competition with each other. To obtain a better description of the relevant states along the reaction coordinate, we calculated the energy profile for the three lowest singlet states and the triplet ground state using the CASPT2 method along the reaction coordinate for the reaction between furan and singlet molecular oxygen obtained with the UM06-2X/AVTZ method. The state-averaged (10e,8o)CASSCF reference wavefunction has a bistability point along the reaction coordinate, which leads to a discontinuous energy surface—see Figure S2; however, the singlet/singlet and singlet/triplet splitting seem not to be affected by this discontinuity (Figure S3). The singlet/triplet splitting calculated at the CASPT2 was utilized as an alternative bypassing scheme, where the singlet/triplet splitting was added to the ROCCSD(T)-F12a/VDZ-F12 triplet surface. The ROCCSD(T)-F12a/VDZ-F12 triplet surface should have a well-behaved single-reference character, and its multireference character is captured using the CASPT2 singlet/triplet splitting. While the maximum of this composite reaction surface is slightly shifted toward the reactant region compared to the TS on the UM06-2X/AVTZ surface (see Figure S4), the energy difference between the two points is only 0.40 kcal/mol. This indicates that both methods have similar potential energy surfaces in the TS region. The electronic energy barrier is calculated to be 13.43 kcal/mol using the composite method, while the UM062X/AVTZ method yields an electronic energy barrier of 17.41 kcal/mol. As shown in Table 1, the UM062X/AVTZ method underestimates the energy of the singlet reactants, which leads to an overestimation of the electronic energy barrier. The electronic energy barrier calculated with the bypassing scheme in Figure 1 is only 3.43 kcal/mol. Considering the reasonable agreement between experimental data and the rate constants shown in Table 2, it is difficult to conclude that the composite method yields an accurate energy barrier for this reaction. Alternatively, the DFT-optimized geometries may give a poor description of the true reaction surface. To investigate this possibility, a CASPT2/AVTZ optimization of the TS was performed. Unfortunately, this TS could not be found.

The reasonable performance of the bypassing scheme outlined in Figure 1 with the furan model system encouraged us to look at a range of systems to test the bypassing approach, with the reasoning that such a test could reveal whether the agreement with literature was fortuitous and whether the approach is physically meaningful. As the furan results were only marginally affected by the choice of DFT method and as the ωB97XD/AVTZ calculation did not appear to be affected by spin contamination, the ωB97XD/AVTZ functional was chosen for further optimization along with the M06-2X because this functional has often been used for similar systems.

3.3 | Pyrrole, 2-methylpyrrole, and 2,5-dimethylpyrrole

TS structures were found for pyrrole, 2-methylpyrrole, and 2,5-dimethylpyrrole (Figure 4). The TSs connect the reactants with the products in a concerted mechanism similar to their furan analogs. As shown in Table 3, the UωB97XD/AVTZ method does not show any spin contamination in the TS, and the T_1 diagnostics are all lower than 0.02, justifying the use of a single-reference method for the TS. The energy barriers are lowered when a hydrogen is exchanged with a methyl group in the pyrrol moiety, in qualitative agreement with the furan system. The energy barrier is observed to become negative for 2-methylpyrrol and 2,5-dimethylpyrrol. TST breaks down when the energy barrier becomes negative, and ideally, other methods should be applied when calculating such a rate constant. However, for the sake of comparison, the rate constants were calculated using traditional TST (without tunneling correction) for the systems with negative barriers. Experimental rate constants have, to our knowledge, only been determined for the 2,5-dimethylpyrrole reaction $k(298\ \text{K}) = 1.66 \times 10^{-13}\ \frac{\text{cm}^3}{\text{s}}$. The calculated rate constants are seen to be 20 to 60 times higher than the experimentally determined ones. The fact that the calculated rates are faster than the experiment can be attributed to their negative energy barriers, which lead to a nonphysical enhancement of the rate constant.

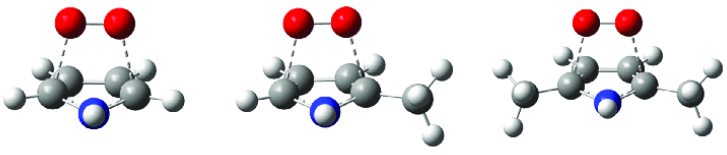

FIGURE 4 Transition state (TS) structure of pyrrol (left), 2-methylpyrrol (middle), and 2,5-dimethylpyrrol (right), calculated at RωB97XD/AVTZ level of theory

TABLE 3 Spin contaminations, T_1 diagnostic, and energy barriers including zero-point vibrational energy (ZPVE) in kcal/mol and rate constants in $\frac{cm^3}{s}$ calculated at CCSD(T)-F12a/VDZ-F12//DFT/AVTZ level of theory using the known singlet/triplet splitting in molecular oxygen

Pyrrole + $^1O_2$	$\langle S^2\rangle$	T_1	E_0 $(\frac{kcal}{mol})$	k $(\frac{cm^3}{s})$	Exp.
RωB97XD	0	0.017	2.57	1.47×10^{-16}	
RM06-2X	0	0.016	2.88	8.81×10^{-17}	
2-Methylpyrrole +$^1O_2$	$\langle S^2\rangle$	T_1	E_0 $(\frac{kcal}{mol})$	k $(\frac{cm^3}{s})$	Exp.
RωB97XD	0	0.016	−0.70	2.95×10^{-14}	
RM06-2X	0.11	0.015	−0.37	1.79×10^{-14}	
UM06-2X	0.02	0.015	−0.44	1.92×10^{-14}	
2,5-Dimethylpyrrole +$^1O_2$	$\langle S^2\rangle$	T_1	E_0 $(\frac{kcal}{mol})$	k $(\frac{cm^3}{s})$	Exp.[29]
RωB97XD	0	0.015	−3.58	3.55×10^{-12}	1.66×10^{-13}
RM06-2X	0.44	0.014	−3.70	5.58×10^{-12}	
UM06-2X	0.07	0.015	−3.43	3.19×10^{-12}	

FIGURE 5 Transition state (TS) structure of cyclopentadiene calculated at RωB97XD/AVTZ level of theory

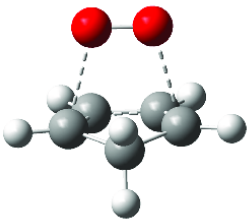

TABLE 4 Spin contaminations, T_1 diagnostic, and energy barriers including zero-point vibrational energy (ZPVE) in kcal/mol and rate constants in $\frac{cm^3}{s}$ calculated at CCSD(T)-F12a/VDZ-F12//DFT level of theory using the known singlet/triplet splitting in molecular oxygen

Cyclopentadiene + $^1O_2$	$\langle S^2\rangle$	T_1	E_0 $(\frac{kcal}{mol})$	k $(\frac{cm^3}{s})$
RωB97XD	0	0.015	3.87	3.90×10^{-17}
RM06-2X	0.61	0.015	2.96	1.14×10^{-16}
UωB97XD	0.26	0.016	2.06	5.33×10^{-16}
UM06-2X	0.25	0.016	3.11	1.87×10^{-16}
Exp.[27]				5.81×10^{-16}

The negative energy barrier could be explained by the existence of a pre-reactive exiplex with a lower energy than the TS. An exiplex was found in the Uω97XD/AVTZ optimization; however, the Uω97XD/AVTZ wavefunction was found to be heavily spin contaminated with $\langle S^2\rangle \approx 1$. The heavy spin contamination in this region of the reaction surface prohibits utilizing the bypassing scheme outlined in Figure 1. We conclude that a full multireference treatment would be necessary in order to include the exiplex in the kinetic model. Reaction enthalpies close to zero are often found for reactions of singlet oxygen in solution; in this case, entropy, rather than the enthalpy, was found to control the reactivity of singlet oxygen.[25]

3.4 | Cyclopentadiene

Cyclopentadiene was selected because experimental data are available for this system, and it is expected to follow a 1,4-cyclo-addition mechanism, as for the furan and pyrrole derivates. The optimized TS obtained at the RωB97XD/AVTZ level of theory is shown in Figure 5. The obtained TSs connect the reactants directly to the product in a concerted reaction. Table 4 shows that no spin contamination is observed for the RωB97XD/AVTZ-optimized TS and that the T_1 diagnostics are lower than 0.02. Again, the multireference character is lost in the TS when optimized using the RωB97XD/AVTZ method. Two different TSs were optimized using the UωB97XD/AVTZ method. One of them is identical to the TS obtained with RωB97XD/AVTZS, and the other has shorter C-O bonds with a geometry more similar to the product. This second TS possess some spin contamination with an $\langle S^2\rangle$ value of 0.27. As it was not possible to find a second TS at the RωB97XD/AVTZ level of theory, we conclude that the second TS is an artifact arising from spin contamination of the wavefunction, which leads to an artificial lowering of the energy over

some part of the potential energy surface. The TS found at the RM06-2X/AVTZ level of theory is more reactant-like compared to the one optimized with the UM06-2X/AVTZ method. Here, we again observe the trend seen in ωB97XD/AVTZ, where the RDFT method finds an earlier TS compared to UDFT. This general trend is also observed for the furan and pyrrole derivatives. The excellent agreement with experimental rates observed for the UωB97XD/AVTZ-calculated rates may simply be due to a cancellation of errors. The RωB97XD/AVTZ-calculated rate constant is 15 times slower than the experimentally determined one. The RωB97XD/AVTZ-calculated rate constant shows the worst agreement with experiment; however, from a computational point of view, it seems to be the most reliable result as no spin contamination is observed for the TS, and the T_1 diagnostic is reasonably low.

3.5 | Temperature dependence

The temperature dependencies of the calculated TST rate constants were calculated and compared to those obtained by Ashford and Ogryzlo to validate the quality of model. As shown in Figure S5, the calculated rates seem to predict the temperature dependencies reasonably well in the interval (298-500 K). In Figure S6, the energy barriers are manually changed by less than 1.5 kcal/mol so that the calculated rate constants match the experimental ones at 298 K. When the temperature is increased to 500 K, the experimentally determined rate constants increase to approximately twice the calculated ones. This result shows that, while the TST model performs reasonably well in predicting the temperature dependencies, it tends to underestimate it. It also shows that the activation barrier for these systems is the most important parameter to be determined in order to obtain accurate rate constants.

4 | CONCLUSION

The rate constants for the reactions between singlet oxygen and seven different reactants are calculated by bypassing the multireference character of singlet oxygen, by performing electronic structure calculations on the triplet state of molecular oxygen, and then adding the experimentally determined energy difference between the two states to obtain the effective energy of the singlet state. All the optimized TSs have low T_1 diagnostics, indicating that the inherent multireference character of singlet oxygen is lost in the TS as the degeneracies of the molecular orbitals are lost at the TSs. The calculated rates are all within a factor of 15 of the experimentally determined rate constants (excluding the nonphysical results obtained from 2,5-dimethylpyrrole). We believe that the accuracy could be further improved by going beyond the TS approximation.

We have tried to perform variational TST calculations on the system to go beyond TST; however, the poor description of singlet oxygen by (R/U)DFT becomes more pronounced when going from the TS toward reactants. This fact has prevented us from obtaining converged reaction paths at the variational transition state theory (VTST) level of theory, and we are working to resolve this issue.

Most of the calculated rate constants were lower than the experimentally determined rate constants, which could indicate that there is a systematic error in either the calculation or the experiments. Care should be taken when selecting the DFT method for optimizations. UDFT seems to be influenced by spin contamination, and artificial TSs can arise as a result of the spin contamination. The agreement with experimentally determined rates is reasonable for both RDFT and UDFT, and we recommend using the RωB97XD functional to optimize TSs for 1,4-cyclo-addition reactions involving singlet oxygen as this functional seems to be the least spin contaminated. We also recommend refining the energy with a single-point CCSD(T)-F12a/VDZ-F12 calculation because the pure DFT energies show huge variations for different functionals. We do not recommend using the approximate spin projection method in connection with DFT energies for calculating rate constants for systems involving singlet molecular oxygen as the energy variation is up to 8.16 kcal/mol across different DFT functionals, compared to 2 kcal/mol when the energy is refined with CCSD(T)-F12a/VDZ-F12 single-point calculations. The approximate spin-projected energy barriers at the M06-2X/AVTZ level of theory are in best agreement with the CCSD(T)-F12a/VDZ-F12 barrier, so we recommend using this functional when an approximate spin-projected method is needed for systems involving singlet molecular oxygen.

The proposed bypassing of the multireference character of singlet oxygen yields a straightforward method for calculating rate constants without the complication of multireference calculations. The reasonable performance for calculating rate constants for the various methods and with different chemical systems shows that the multireference character in singlet oxygen can be effectively bypassed by performing the calculations with the triplet state of molecular oxygen and simply adding the experimentally determined singlet/triplet energy splitting to obtain the energy of singlet oxygen. We emphasize that the bypassing scheme relies on a well-behaved TS without a strong multireference character. Low spin contamination and T1 diagnostic are paramount in validating the quality of the bypassing scheme. In this work, we have only tested the bypassing scheme on the 1,4-cyclo-addition mechanism. Further work is needed to validate this approach for other singlet oxygen reaction mechanism.

ACKNOWLEDGMENTS

This work was supported by the Center for Exploitation of Solar Energy, Department of Chemistry, University of Copenhagen, Denmark.

AUTHOR CONTRIBUTIONS

Malte F. Jespersen: Conceptualization; data curation; formal analysis; investigation; methodology. **Solvejg Jørgensen:** Conceptualization; investigation. **Matthew S. Johnson:** Conceptualization; investigation; writing-review and editing. **Kurt V. Mikkelsen:** Conceptualization; formal analysis; investigation; methodology; project administration; supervision; writing-review and editing.

ORCID

Malte F. Jespersen https://orcid.org/0000-0002-8549-2694
Kurt V. Mikkelsen https://orcid.org/0000-0003-4090-7697

REFERENCES

[1] N. Lane, *Oxygen: The Molecule that Made the World*, 1st ed., Oxford University Press, Oxford **2002**.
[2] M. Bregnhøj, M. Westberg, B. F. Minaev, P. R. Ogilby, *Acc. Chem. Res.* **2017**, *50*, 1920.
[3] G. Herzberg, *Molecular Spectra and Molecular Structure. I Spectra of Diatomic Molecules*, 2nd ed., Van Nostrand Reinhold, New York **1950**.
[4] R. Gerdes, D. Wöhrle, W. Spiller, G. Schneider, G. Schnurpfeil, G. Schulz-Ekloff, *J. Photochem. Photobiol. A Chem.* **1997**, *111*, 65.
[5] V. Iliev, L. Prahov, L. Bilyarska, H. Fischer, G. Schulz-Ekloff, D. Wöhrle, L. Petrov, *J. Mol. Catal. A: Chem.* **2000**, *151*, 161.
[6] R. Bonnett, *Chem. Soc. Rev.* **1995**, *24*, 19.
[7] M. C. DeRosa, R. J. Crutchley, *Coord. Chem. Rev.* **2002**, *233*, 351.
[8] H. H. Wasserman, J. L. Ives, *Tetrahedron* **1981**, *37*, 1825.
[9] B. C. Faust, J. M. Allen, *J. Geophys. Res. Atmos.* **1992**, *97*, 12913.
[10] K. Yamaguchi, S. Yamanaka, J. Shimada, H. Isobe, T. Saito, M. Shoji, Y. Kitagawa, M. Okumura, *Int. J. Quantum Chem.* **2009**, *109*, 3745.
[11] L. B. Harding, W. A. Goddard III., *J. Am. Chem. Soc.* **1980**, *102*, 439.
[12] M. N. Alberti, M. Orfanopoulos, *Chem. Eur.* **2010**, *16*, 9414.
[13] D. A. Singleton, C. Hang, M. J. Szymanski, M. P. Meyer, A. G. Leach, K. T. Kuwata, J. S. Chen, A. Greer, C. S. Foote, K. Houk, *J. Am. Chem. Soc.* **2003**, *125*, 1319.
[14] M. J. Dewar, W. Thiel, *J. Am. Chem. Soc* **1977**, *99*, 2338.
[15] M. W. Schmidt, M. S. Gordon, *Annu. Rev. Phys. Chem.* **1998**, *49*, 233.
[16] S. Yamanaka, T. Kawakami, H. Nagao, K. Yamaguchi, *Chem. Phys. Lett.* **1994**, *231*, 25.
[17] T. Saito, S. Nishihara, Y. Kataoka, Y. Nakanishi, Y. Kitagawa, T. Kawakami, S. Yamanaka, M. Okumura, K. Yamaguchi, *J. Phys. Chem. A* **2010**, *114*, 7967.
[18] J. Al-Nu'airat, M. Altarawneh, X. Gao, P. R. Westmoreland, B. Z. Dlugogorski, *J. Phys. Chem. A* **2017**, *121*, 3199.
[19] T. Saito, S. Nishihara, Y. Kataoka, Y. Nakanishi, T. Matsui, Y. Kitagawa, T. Kawakami, M. Okumura, K. Yamaguchi, *Chem. Phys. Lett.* **2009**, *483*, 168.
[20] F. Sevin, M. L. McKee, *J. Am. Chem. Soc.* **2001**, *123*, 4591.
[21] A. G. Leach, K. Houk, *Chem. Commun.* **2002**, 1243.
[22] M. Bobrowski, A. Liwo, S. Oldziej, D. Jeziorek, T. Ossowski, *J. Am. Chem. Soc.* **2000**, *122*, 8112.
[23] M. A. McCarrick, Y. D. Wu, K. Houk, *J. Org. Chem.* **1993**, *58*, 3330.
[24] W. Fudickar, T. Linker, *J. Phys. Org. Chem.* **2019**, *32*, e3951.
[25] A. Gorman, G. Lovering, M. Rodgers, *J. Am. Chem. Soc.* **1979**, *101*, 3050.
[26] A. Gorman, I. Hamblett, C. Lambert, B. Spencer, M. Standen, *J. Am. Chem. Soc* **1988**, *110*, 8053.
[27] R. Ashford, E. Ogryzlo, *Can. J. Chem.* **1974**, *52*, 3544.
[28] R. E. Huie, J. T. Herron, *Int. J. Chem. Kinet.* **1973**, *5*, 197.
[29] E. Fiedler, W. Hack, *Int. J. Chem. Kinet.* **1991**, *23*, 925.
[30] M. J. Frisch, G. W. Trucks, H. B. Schlegel, G. E. Scuseria, M. A. Robb, J. R. Cheeseman, G. Scalmani, V. Barone, G. A. Petersson, H. Nakatsuji, X. Li, M. Caricato, A. V. Marenich, J. Bloino, B. G. Janesko, R. Gomperts, B. Mennucci, H. P. Hratchian, J. V. Ortiz, A. F. Izmaylov, J. L. Sonnenberg, D. Williams-Young, F. Ding, F. Lipparini, F. Egidi, J. Goings, B. Peng, A. Petrone, T. Henderson, D. Ranasinghe, V. G. Zakrzewski, J. Gao, N. Rega, G. Zheng, W. Liang, M. Hada, M. Ehara, K. Toyota, R. Fukuda, J. Hasegawa, M. Ishida, T. Nakajima, Y. Honda, O. Kitao, H. Nakai, T. Vreven, K. Throssell, J. A. Montgomery Jr., J. E. Peralta, F. Ogliaro, M. J. Bearpark, J. J. Heyd, E. N. Brothers, K. N. Kudin, V. N. Staroverov, T. A. Keith, R. Kobayashi, J. Normand, K. Raghavachari, A. P. Rendell, J. C. Burant, S. S. Iyengar, J. Tomasi, M. Cossi, J. M. Millam, M. Klene, C. Adamo, R. Cammi, J. W. Ochterski, R. L. Martin, K. Morokuma, O. Farkas, J. B. Foresman, D. J. Fox, *Gaussian 16, Revision A.03*, Gaussian Inc, Wallingford, CT **2016**.
[31] R. A. Kendall, T. H. Dunning Jr., R. J. Harrison, *J. Chem. Phys.* **1992**, *96*, 6796.
[32] J. D. Chai, M. H. Gordon, *Phys. Chem. Chem. Phys.* **2008**, *10*, 6615.
[33] A. D. Becke, *J. Chem. Phys.* **1993**, *98*, 5648.
[34] Y. Zhao, D. G. Truhlar, *Theory. Chem. Acc.* **2008**, *120*, 215.
[35] H.-J. Werner, P. J. Knowles, G. Knizia, F. R. Manby, M. Schütz, P. Celani, W. Györffy, D. Kats, T. Korona, R. Lindh, A. Mitrushenkov, G. Rauhut, K. R. Shamasundar, T. B. Adler, R. D. Amos, A. Bernhardsson, A. Berning, D. L. Cooper, M. J. O. Deegan, A. J. Dobbyn, F. Eckert, E. Goll, C. Hampel, A. Hesselmann, G. Hetzer, T. Hrenar, G. Jansen, C. Köppl, Y. Liu, A. W. Lloyd, R. A. Mata, A. J. May, S. J. McNicholas, W. Meyer, M. E. Mura, A. Nicklass, D. P. O'Neill, P. Palmieri, D. Peng, K. Pflüger, R. Pitzer, M. Reiher, T. Shiozaki, H. Stoll, A. J. Stone, R. Tarroni, T. Thorsteinsson, M. Wang, *MOLPRO, Version 2012.1, A Package of Ab Initio Programs*, MOLPRO, Cardiff, UK **2012**.
[36] G. Knizia, T. B. Adler, H.-J. Werner, *J. Chem. Phys* **2009**, *130*, 054104.
[37] H. Eyring, *J. Chem. Phys.* **1935**, *3*, 107.
[38] C. Eckart, *Phys. Rev.* **1930**, *35*, 1303.
[39] J. Al-Nu'airat, B. Z. Dlugogorski, X. Gao, N. Zeinali, J. Skut, P. R. Westmoreland, I. Oluwoye, M. Altarawneh, *Phys. Chem. Chem. Phys.* **2019**, *21*, 171.
[40] T. J. Lee, P. R. Taylor, *Int. J. Quantum Chem.* **1989**, *36*, 199.
[41] C. F. Goldsmith, S. J. Klippenstein, W. H. Green, *Proc. Combust. Inst.* **2011**, *33*, 273.

[42] D. G. Truhlar, B. C. Garrett, *Acc. Chem. Res.* **1980**, *13*, 440.
[43] T. N. Karsili, B. Marchetti, *J. Chem. Phys. A* **2019**, *124*, 498.
[44] B. Marchetti, T. N. Karsili, *Chem. Commun.* **2016**, *52*, 10996.
[45] F. Thorning, F. Jensen, P. R. Ogilby, *J. Phys. Chem. B* **2020**, *124*, 2245.

SUPPORTING INFORMATION

Additional supporting information may be found online in the Supporting Information section at the end of this article.

How to cite this article: Jespersen MF, Jørgensen S, Johnson MS, Mikkelsen KV. Bypassing the multireference character of singlet molecular oxygen, part 1:1,4-cyclo-addition. *Int J Quantum Chem*. 2021;121:e26523. https://doi.org/10.1002/qua.26523